Structures and Properties of Injection Moldings of Crystallization Nucleator-Added Polypropylenes. I. Structure–Property Relationships

MITSUYOSHI FUJIYAMA and TETSUO WAKINO

Polymer Development Laboratory, Tokuyama Soda Co., Ltd., Tokuyama-shi, Yamaguchi-ken 745, Japan

SYNOPSIS

Flexural test specimens were injection-molded from polypropylenes added with 0.5 wt % of calcium carbonate, talc, *p-tert*-dibutyl-benzoic acid monohydroxy aluminum, or *p*-dimethyl-benzylidene sorbitol under cylinder temperatures of 200–320°C. Properties such as flexural modulus, flexural strength, heat distortion temperature, Izod impact strength, hardness, and mold shrinkage and higher-order structures such as crystalline texture, crystallinity, a^*-axis-oriented component fraction, and degree of crystalline orientation were measured and structure–property relationships were studied. By the addition of crystallization nucleators, the flexural modulus, flexural strength, heat distortion temperature, hardness, and mold shrinkage were increased and Izod impact strength was decreased. The degrees of crystalline orientation such as the orientation fraction OF and *c*-axis orientation function f_c were increased by the addition of nucleators. The degree of the increase was higher as the crystallization temperature was higher. Close relationships were observed between some properties and the degrees of crystalline orientation.

INTRODUCTION

When crystallization nucleators are added to crystalline polymers, the following effects are expected[1–3]: (i) improvement of transparency of molded articles, (ii) improvement of processing cycle or spinnability, (iii) improvement of rigidity of molded articles or filaments, (iv) improvement of dimensional precision, (v) improvement of gloss, and (vi) prevention of sink. As crystallization nucleators for polypropylene, talc,[4–6] aluminum salts of benzoic acids,[6–9] and dibenzylidene sorbitols[3,6,7,10–12] are especially effective and studies have been concentrated on them.

This paper is concerned with studies on structures and properties and structure–property relationships of injection moldings of crystallization nucleator-added polypropylenes. Polypropylene was fixed and effects of addition of talc, *p-tert*-dibutyl benzoic acid monohydroxy aluminum, or *p*-dimethylbenzylidene sorbitol, which are widely and frequently used and of calcium carbonate, which shows almost no nucleating effect and hence was used for comparison were studied. Nucleator content was fixed at 0.5 wt %. Flexural test specimens were injection-molded by varying cylinder temperature at 200–320°C. Properties such as flexural modulus, flexural strength, heat distortion temperature, Izod impact strength, hardness, and mold shrinkage and higher-order structures such as crystalline texture, crystallinity, a^*-axis-oriented component fraction, and degrees of crystalline orientation were measured and relationships between flexural modulus, flexural strength, and mold shrinkage and degrees of crystalline orientation were studied.

EXPERIMENTAL

Samples

Polypropylene used was homoisotactic polypropylene powder, Grade PN 120, which was produced by Tokuyama Soda Co., Ltd. and had a melt flow index (MFI) of 2 dg/min.

Journal of Applied Polymer Science, Vol. 42, 2739–2747 (1991)
 CCC 0021-8995/91/102739-09$04.00

Crystallization nucleators used were Stavigot 15A (hereinafter abbreviated as CC), which was a precipitated calcium carbonate produced by Shiraishi Industry Co., Ltd. and surface-treated with an aliphatic acid and had an average diameter of 0.2 μm, Crown Talc-Z (hereinafter abbreviated as TC), which was a talc produced by Matsumura Industry Co., Ltd. and had an average diameter of 10 μm, *p-tert*-dibutyl-benzoic acid monohydroxy aluminum (hereinafter abbreviated as BA) produced by Shell Chemical Co., Ltd., and Gelall MD (hereinafter abbreviated as GA) which was *p*-dimethyl-benzylidene sorbitol produced by New Japan Chemical Co., Ltd.

The polypropylene powder was mixed with 0.5 wt % of nucleators for 5 min in a 100-L Supermixer, extruded by a CCM extruder with a vent at a kneader temperature of 190°C and an extruder temperature of 220°C into a strand which was cut into pellets of about 3 mm size by an automatic cutter. Hereinafter, the sample without nucleator is called PP, the samples with CC, TC, BA, and GA are called CC, TC, BA, and GA, respectively.

Figure 1 shows the dependence of crystallization temperatures T_c of nucleator-added polypropylenes on the cooling rate. A sheet 0.3 mm thick was molded on a hot plate. It was put into a sample pan, and, after it was melted in the furnace of a differential scanning calorimeter, Perkin-Elmer DSC-BI, in a nitrogen atmosphere at 230°C for 10 min, it was cooled at various rates. The peak temperature of the exothermic curve was taken as T_c. Increases in T_c by nucleator additions are CC; 1–2°C, TC; 9–11°C, BA; 15–16°C, and GA; 16–17°C, and the latter shows more notable nucleating effect.

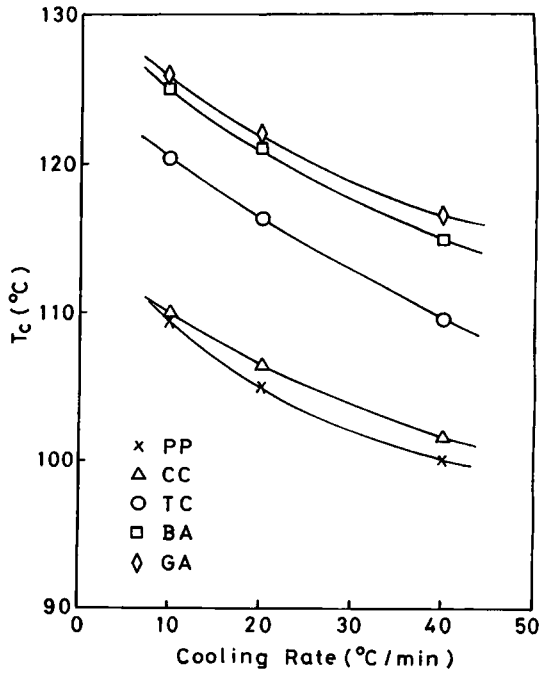

Figure 1 Dependence of crystallization temperature T_c on cooling rate.

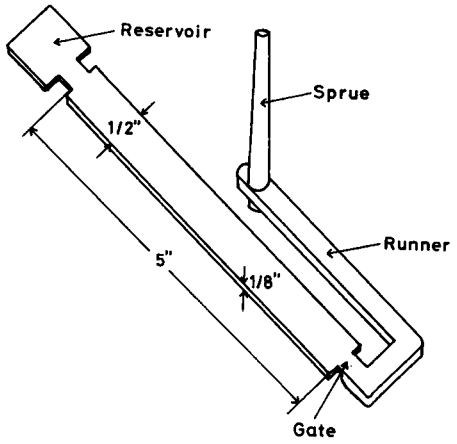

Figure 2 Shape of test specimen.

Injection Molding

Flexural test specimens (ASTM D790) were injection-molded using an 8 oz NIKKO ANKERWERK V22A-120 type reciprocating-screw injection molding machine. The shape of the test specimen is shown in Figure 2. A polymer reservoir was provided to make resin flow in the specimen uniform. The gate size measured 7.0 mm wide, 1.5 mm thick, and 3.0 mm long. The sprue was a truncated cone with 5.4 mm inlet diameter, 7.4 mm outlet diameter, and 45 mm long and the runner measured 7.0 mm wide, 4.5 mm thick, and 100 mm long. Since cylinder temperature affects the degree of molecular orientation of the product and its mechanical properties more than any other injection molding conditions,[13] injection molding was carried out, varying cylinder temperature only and keeping all other conditions constant. Table I lists injection molding conditions adopted. The cylinder temperatures were represented by the temperature of the metering zone (MH3) at the extreme end.

Measurements of Properties

After flexural test specimens were conditioned under a constant temperature and humidity at 23°C and 50% RH for more than 2 weeks after they were molded, flexural modulus and flexural strength were measured with a Shimazu Autograph AG-5000A ac-

Table I Injection Molding Conditions

Expt No	Cylinder Temperature (°C)				Injection Pressure (kg/cm^2)	Injection Speed (cc/s)	Mold Temperature (°C)	Cooling Time (s)
	MH1[a]	MH2[b]	MH3[c]	DH[d]				
1	160	190	200	190	500	13.5	40	40
2	160	220	240	220	500	13.5	40	40
3	160	250	280	250	500	13.5	40	40
4	160	280	320	280	500	13.5	40	40

[a] Feed zone.
[b] Compression zone.
[c] Metering zone.
[d] Die head.

cording to the ASTM D790. Heat distortion temperature was measured under a stress of 4.6 kg/cm^2 according to the ASTM D648. Izod impact strength was measured with molded-in notched specimens according to the ASTM D256. Rockwell hardness on B-scale was measured at the central parts of flexural specimens according to the ASTM D785. Length L in the flow direction (MD) of flexural specimen was measured with a micrometer and mold shrinkage was calculated by the following equation:

$$\text{mold shrinkage}\ (\%) = \frac{L_0 - L}{L_0} \times 100 \qquad (1)$$

where L_0 is the length of the mold cavity.

Structural Analyses

Thin sections about 0.1 mm thick were sliced from the central parts of the specimens perpendicular to the flow direction (MD) with a microtome and their crystalline textures were observed with a polarizing microscope, Olympus PM-6, under a magnification of 20×.

Wide-angle X-ray diffraction patterns were taken at the central parts of the specimens by setting their MD in accord with the meridian using a Rigaku Denki RU-200 diffractometer with Ni-filtered Cu-K_α radiation at a sample-to-film distance of 45 mm. They showed that fiber patterns of the mixed c-axis and a^*-axis orientations overlapped on Debye rings. Using a goniometer, 2θ scans were carried out at a scan speed of 4°/min and azimuthal scans of the (110) and (040) plane reflections were carried out at a scan speed of 8°/min. Figure 3 exemplifies the 2θ scan curve and (110) plane and (040) plane azimuthal scan curves of a specimen molded from GA at a cylinder temperature of 240°C. In order to evaluate the proportions of the c-axis-oriented component and a^*-axis-oriented component, the following procedure was carried out: A base line (BL2) was drawn horizontally at the bottom of the azimuthal scan curve of the (110) reflection; the area around an azimuthal angle of 0° above the base line was taken as C and the area around an azimuthal angle of 90° above the base line was taken as A^*; the c-axis-oriented component fraction [C] and a^*-axis-oriented component fraction [A^*] were defined as follows:

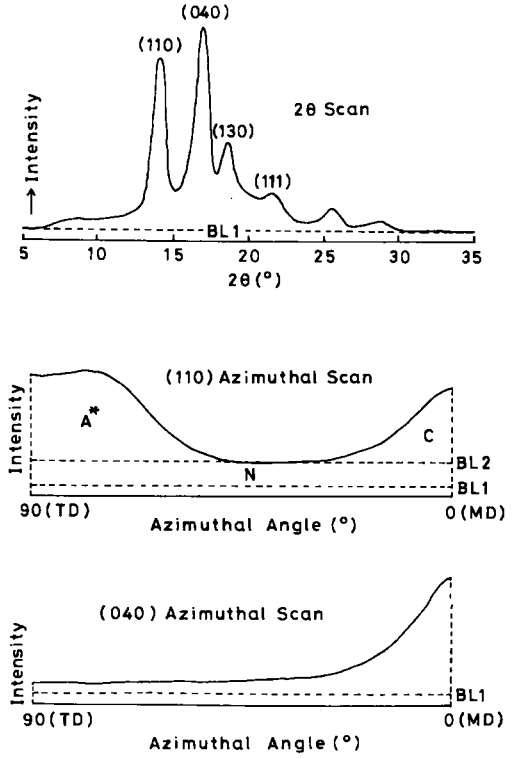

Figure 3 2θ scan curve and (110) and (040) plane azimuthal scan curves of specimen molded from GA at cylinder temperature of 240°C.

$$[C] = \frac{C}{C + A^*} \tag{2}$$

$$[A^*] = \frac{A^*}{C + A^*} \tag{3}$$

Although there is no assurance that the absolute amounts of c-axis-oriented and a^*-axis-oriented components can be rigorously evaluated by $[C]$ and $[A^*]$, a relative comparison may be made by them when raw resin and/or molding conditions are changed.

Since injection-molded polypropylenes show the mixed c-axis and a-axis orientations, the c-axis-oriented component and the a^*-axis-oriented component cancel each other at the calculation of the orientation functions, and hence it is not very appropriate to evaluate the degree of crystalline orientation from the orientation functions. Therefore, a quantity OF (orientation fraction) was defined as follows and was used as a measure of crystalline orientation:

$$\mathrm{OF} = \frac{C + A^*}{C + A^* + N} \tag{4}$$

where N (nonoriented) is the area enveloped by the BL2 and the BL1, which is the base line of the 2θ scan curve, in the (110) plane azimuthal scan curve in Figure 3.

Also, the crystalline orientation functions (a^*-axis orientation function f_{a^*}, b-axis orientation function f_b, and c-axis orientation function f_c) were calculated from the (110) plane and (040) plane azimuthal scan curves according to the Wilchinsky's method.[14]

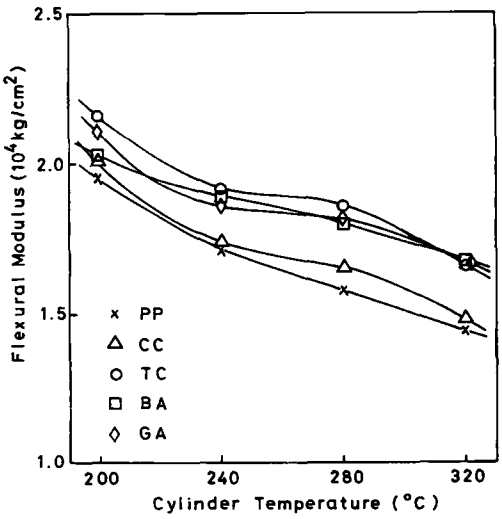

Figure 4 Dependence of flexural modulus on cylinder temperature.

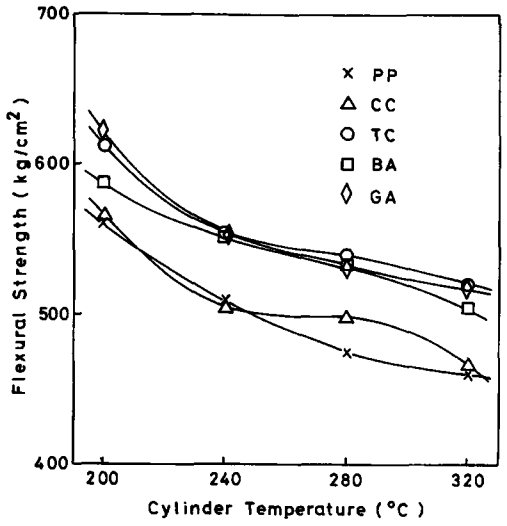

Figure 5 Dependence of flexural strength on cylinder temperature.

2θ scans were carried out at the central parts of the specimens using a rotating specimen table and the crystallinities X_c were calculated according to the Weidinger and Hermans method.[15]

RESULTS AND DISCUSSION

Properties

Figure 4 shows the dependence of flexural modulus (FM) on cylinder temperature. FM decreases with increasing cylinder temperature and is increased by the addition of nucleators. CC has almost no effect of increasing FM, and TC, BA, and GA have a similar effect. From this, it can be said that the rigidity of injection molding is improved by the addition of nucleators.

Figure 5 shows the dependence of flexural strength on cylinder temperature. Similar behaviors to those of flexural modulus are observed.

Figure 6 shows the dependence of heat distortion temperature (HDT) on cylinder temperature. The effect of increasing HDT is in the order of BA > TC > GA > CC. The addition of BA improves HDT by 15–20°C.

Figure 7 shows the dependence of Izod impact strength (IIS) on cylinder temperature. The addition of CC or TC increases IIS little or a little. The addition of BA considerably decreases IIS and the addition of GA notably decreases IIS.

Figure 8 shows the dependence of hardness on

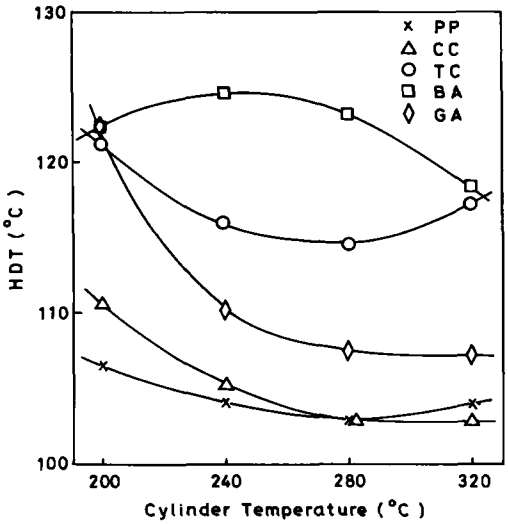

Figure 6 Dependence of heat distortion temperature (HDT) on cylinder temperature.

cylinder temperature. The addition of CC scarcely changes hardness and the addition of TC, BA, or GA increases hardness. The effect of increasing hardness is higher as T_c is higher.

Figure 9 shows the dependence of mold shrinkage (MS) on cylinder temperature. The addition of TC decreases MS and the addition of CC, BA, or GA increases MS. Although the GA specimens show high MS, the change of MS with cylinder temperature is small.

Higher-Order Structures

Figure 10 shows the changes caused by cylinder temperature to a crystalline texture observed with

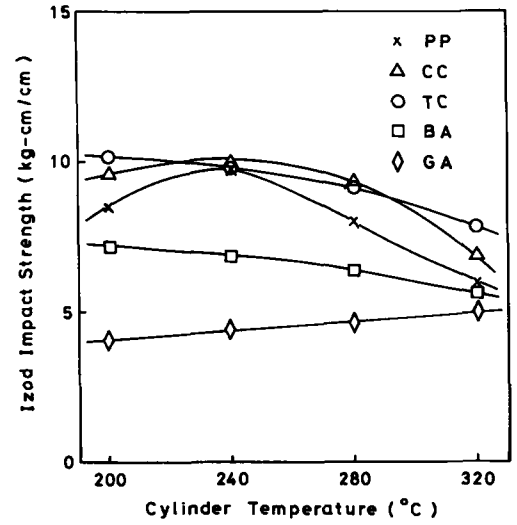

Figure 7 Dependence of Izod impact strength on cylinder temperature.

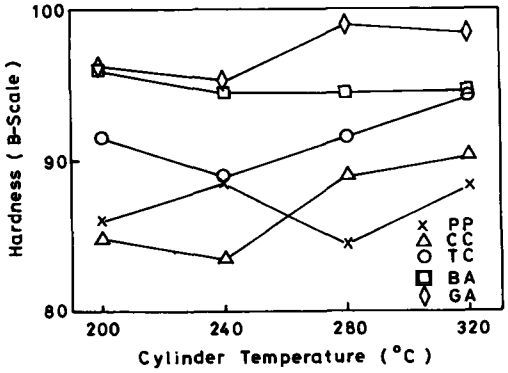

Figure 8 Dependence of hardness on cylinder temperature.

a polarizing microscope. The PP, CC, and TC specimens show clear skin/core structures and the thickness of the skin layer decreases with increasing cylinder temperature. No skin layer is observed for the BA and GA specimens; in particular, the GA specimens show homogeneous textures.

Figure 11 shows the dependence of mean crystallinity X_c on cylinder temperature. X_c is scarcely changed by the addition of CC or BA and is increased by 1–2% by the addition of TC or GA. X_c tends to increase with increasing cylinder temperature, which is because the higher the cylinder temperature, the higher the injected resin temperature, which takes longer time to be cooled and the cooling rate is low.

Figure 12 shows the dependence of the a^*-axis-oriented component fraction $[A^*]$ on cylinder temperature. The CC specimens show nearly similar behaviors to those of the PP specimens and their $[A^*]$'s increase with increasing cylinder temperature. Namely, this means that the fraction of the a^*-axis-oriented component as against to that of the c-axis-oriented component increases with increasing cylinder temperature in injection moldings

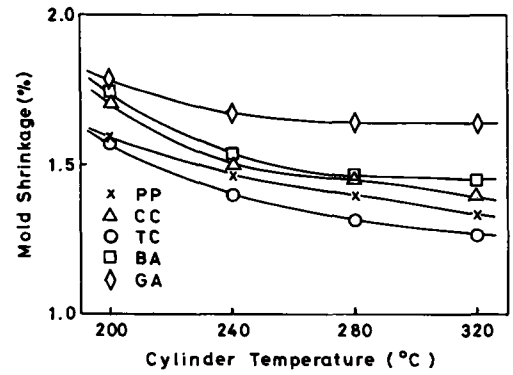

Figure 9 Dependence of mold shrinkage on cylinder temperature.

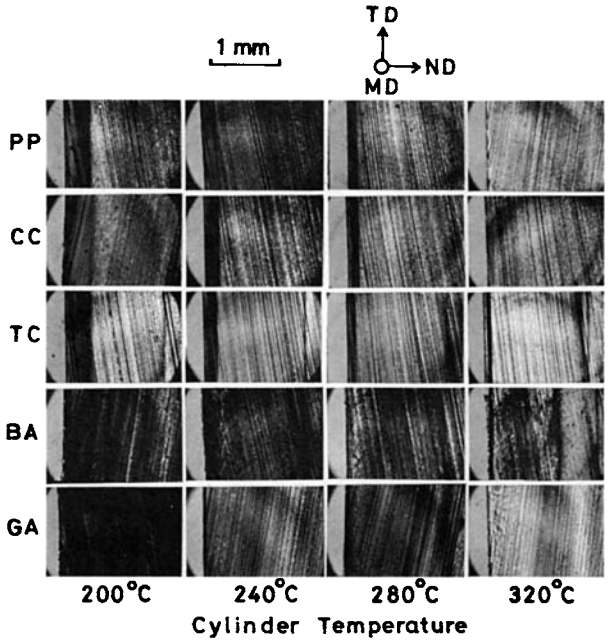

Figure 10 Changes with cylinder temperature, of polarized micrographs of injection moldings of nucleator-added polypropylenes.

of PP and CC. [A^*]'s of the TC and GA specimens scarcely depend on cylinder temperature and are lower than those of the PP specimens. Namely, the addition of TC or GA decreases the a^*-axis-oriented component and increases the c-axis-oriented component. The BA specimens show behaviors intermediate between the PP and CC specimens and the TC and GA specimens.

Figure 13 shows the dependence of the orientation fraction OF on cylinder temperature. OF decreases with increasing cylinder temperature. Although OF's of the CC and TC specimens scarcely differ from those of the PP specimens, OF's of the BA and GA

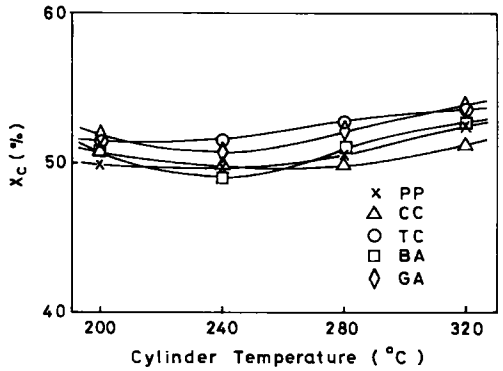

Figure 11 Dependence of crystallinity X_c on cylinder temperature.

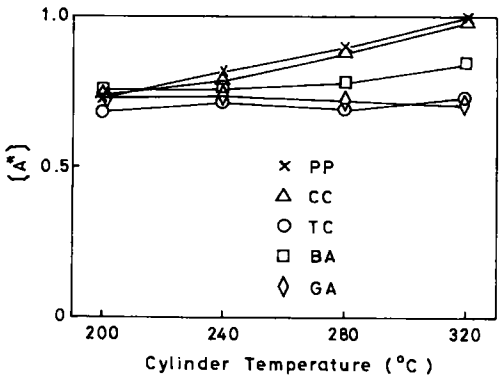

Figure 12 Dependence of a^*-axis-oriented component fraction [A^*] on cylinder temperature.

specimens, in particular, of the GA specimens, are increased largely. From this, it can be said that a small amount (0.5 wt %) of addition of BA or GA largely increases the degree of the crystalline orientation of the injection molding. According to the authors' theory,[16-20] this is because, although the degree of melt orientation (recoverable shear strain) is scarcely changed by the addition of BA or GA, the relaxation time of the recoverable shear strain (the time for recoiling of extended chains) is increased by the addition, in particular, of GA as shown in Figure 13 of the following paper since GA gelates at temperatures below around 190°C,[3] and because the addition of BA or GA promotes sooner solidification since it increases the crystallization temperature as shown in Figure 1.

Figure 14 shows the dependence of the orientation functions on cylinder temperature. The absolute values of the c-axis orientation function f_c and b-axis orientation function f_b decrease with increasing cylinder temperature. The a^*-axis orientation func-

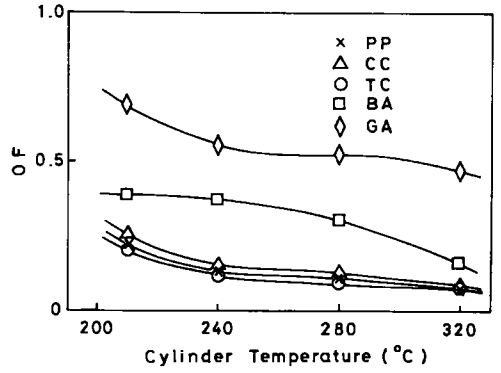

Figure 13 Dependence of orientation fraction OF on cylinder temperature.

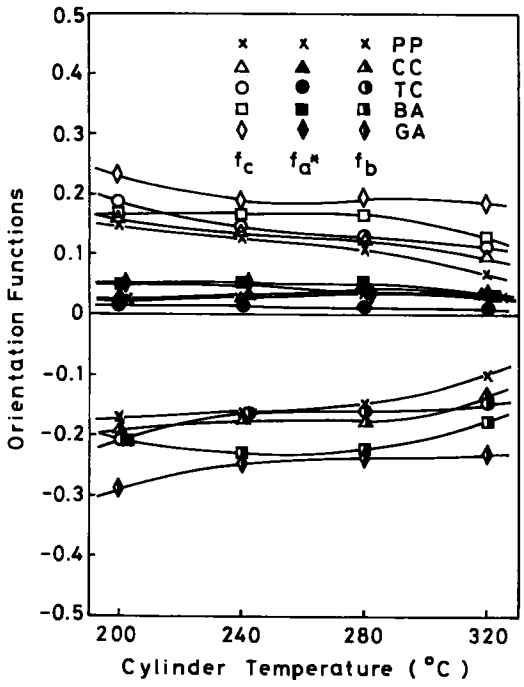

Figure 14 Dependence of crystalline orientation functions on cylinder temperature.

tions f_{a^*} of the PP and CC specimens somewhat increase with increasing cylinder temperature, and f_{a^*}'s of the TC, BA, and GA specimens slightly decrease with increasing cylinder temperature. f_{a^*}'s of the CC specimens are nearly equal to those of the PP specimens. f_{a^*}'s of the BA and GA specimens are slightly higher than those of the PP specimens and f_{a^*}'s of the TC specimens are slightly lower than those of the PP specimens. The order of f_c is GA > BA > TC > CC > PP and is the same as that of the crystallization temperature. The interpretation for this is the same as that for OF.

Structure–Property Relationships

As for the relationship in injection molding between the crystalline orientation and property, studies of the authors on unfilled polypropylenes[16] and particulate-filled polypropylenes[17] have been reported, but there has been no study on crystallization nucleator-added polypropylene.

Figures 15 and 16 show relations between the flexural modulus and mold shrinkage, respectively, and the orientation fraction OF. Between the two, there exist different rectilinear relationships, with positive slopes depending on the kind of nucleator. Similar relationships were obtained between flexural strength and OF. This means that these properties increase with increasing OF and that such a relationship differs depending on the kind of nucleator and cannot be unified only with OF, and the individual character of the sample still remains. This individual character is assumed to be originated from higher-order structures beside crystalline orientation, for example, such as crystallinity, spherulite size, lamella thickness, etc.

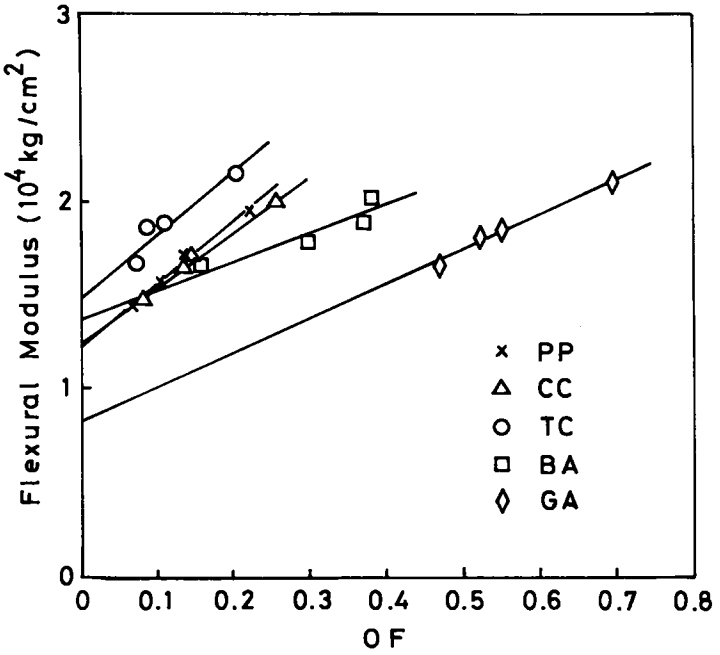

Figure 15 Relation between flexural modulus and orientation fraction OF.

Figure 17 shows relation between the flexural modulus and the c-axis orientation function f_c. The flexural modulus, flexural strength, and f_c are in rectilinear relationships with positive slopes, and the mold shrinkage and f_c is in downward curvilinear relationships. It seems that the properties are in better relationships with OF than with f_c.

CONCLUSIONS

Flexural test specimens were injection-molded from polypropylenes containing 0.5 wt % of calcium carbonate (CC), talc (TC), *p-tert*-dibutyl-benzoic acid monohydroxy aluminum (BA), or Gelall MD (GA) under cylinder temperatures of 200–320°C and properties and higher-order structures and structure–property relationships were studied. The following results were obtained:

1. Property: By the addition of crystallization nucleators, the flexural modulus, flexural strength, heat distortion temperature, hardness, and mold shrinkage are increased and Izod impact strength is decreased.
2. Structure:
   (i) While clear skin/core structures are observed in injection moldings of PP, CC, and TC, no skin layer is observed in those of BA and GA.

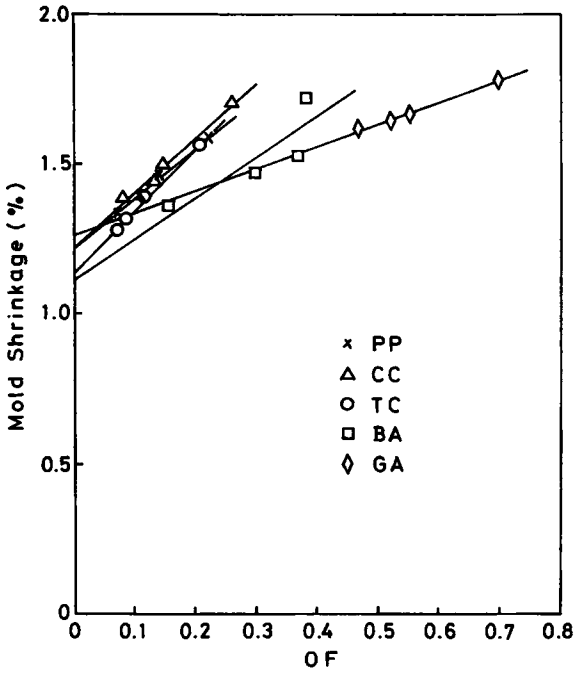

Figure 16 Relation between mold shrinkage and orientation fraction OF.

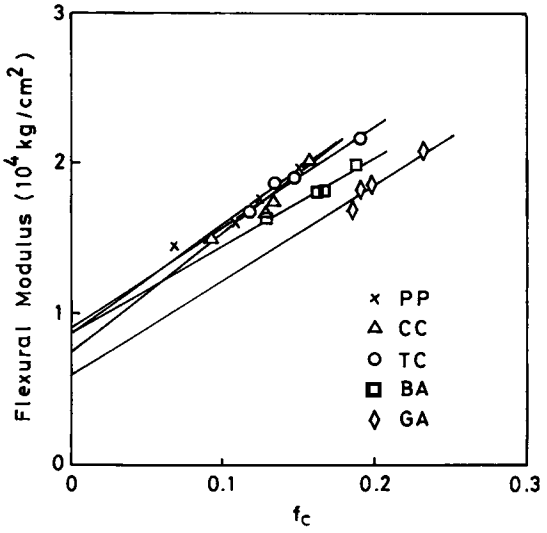

Figure 17 Relation between flexural modulus and c-axis orientation function f_c.

   (ii) The crystallinity X_c is increased by 1–2% by the addition of TC or GA.
   (iii) Although the a^*-axis-oriented component fraction [A^*] is scarcely changed by the addition of CC, it is decreased by the addition of TC, BA or GA.
   (iv) The degrees of crystalline orientation such as the orientation fraction OF and c-axis orientation function f_c are increased by the addition of nucleators. The degree of the increase is higher as the crystallization temperature is higher. This is because the higher the crystallization temperature, the faster the solidification and the less the relaxation of melt orientation (recoverable shear strain).
3. Structure–property relationship: The flexural modulus, flexural strength, and mold shrinkage are in different rectilinear relationships with positive slopes with OF or f_c depending on the kind of nucleator. This means that the higher the crystalline orientation, the higher the flexural modulus, flexural strength, and mold shrinkage.

The authors would like to thank Tokuyama Soda Co., Ltd. for permission to publish this paper.

REFERENCES

1. C. J. Kuhre, M. Wales, and D. E. Doyle, *SPE J.*, **20**(10), 1113 (1964).
2. J. E. Lane, *Bri. Plast.*, **39**, 528 (1966).

3. T. Kobayashi, in *New Technology of Polymer Additives,* CMC, Tokyo, 1988, p. 204.
4. L. Klostermann, *Plastverarbeiter,* **33,** 262 (1982).
5. J. Menczel and J. Varga, *J. Thermal Anal.,* **28,** 161 (1983).
6. H. Nakagawa and H. Sano, *Polym. Prepr. Jpn.,* **33**(4), 680 (1984).
7. K. Tanaka and H. Baba, *Polym. Prepr. Jpn.,* **29**(9), 2011 (1980).
8. K. Ikeda, *Kobunshi Ronbunshu,* **44,** 539 (1987).
9. K. Ikeda, *Kobunshi Ronbunshu,* **46,** 45 (1989).
10. C. C. Carroll, *Package Chall 80's,* 68 (1984), preprint.
11. T. Kobayashi, *Polym. Appl. Jpn.,* **35,** 1 (1986).
12. H. Sano, K. Tanaka, and H. Nakagawa, *Polym. Prepr. Jpn.,* **36**(4), 932 (1987).
13. M. Fujiyama and S. Kimura, *Kobunshi Ronbunshu,* **32,** 581 (1975).
14. Z. W. Wilchinsky, *J. Appl. Phys.,* **31,** 1969 (1960).
15. W. Weidinger and P. H. Hermans, *Makromol. Chem.,* **50,** 98 (1961).
16. M. Fujiyama, *Nihon Reoroji Gakkaishi,* **14,** 152 (1986).
17. M. Fujiyama, Y. Kawasaki, and T. Wakino, *Nihon Reoroji Gakkaishi,* **15,** 191 (1987).
18. M. Fujiyama, Y. Kawasaki, and T. Wakino, *Nihon Reoroji Gakkaishi,* **15,** 203 (1987).
19. M. Fujiyama and T. Wakino, *J. Appl. Polym. Sci.,* to appear.
20. M. Fujiyama and T. Wakino, *J. Appl. Polym. Sci.,* to appear.

Received March 13, 1990
Accepted July 24, 1990